An Improved Sunflower-Inspired Solar Tracking Strategy for Maximizing Photovoltaic Panel Power Generation

Rexel U. Sabran, Arnel C. Fajardo

Abstract*: A previous study proposed a nature-inspired tracking strategy that mimics the solar tracking behavior of sunflowers driven by the light stimulus and the circadian clock. The approach delivered a good tracking performance with an average tracking error of 0.727° under clear, partly cloudy, and cloudy conditions. However, it incurred high tracking errors caused by false detection brought about by the abrupt changes in the amount of solar radiation during realignment. In addition, the scheme also maintained high stepper motor current consumption due to the use of a fixed stepping resolution. To address these issues, the previous tracking routine was modified to direct the search for the sun's position to a range of calculated altitude angles where a fine-tuning process will be performed using current measurements and the adoption of a variable stepping resolution during panel reorientation. Experiments were conducted to measure the performance of the modifications in terms of tracking error, power generation, and stepper motor current consumption. A comparison of the performances between the previous and the modified approaches was done to assess the impact of the proposed improvement. The result of the comparison showed that the modifications significantly improved the overall tracking performance of the strategy.

***Index Terms*: Biomimicry, Solar Tracking, Tracking Strategy, Maximizing PV power generation**

I. INTRODUCTION

Solar energy is an abundant renewable energy resource that provides clean electricity for residential and commercial use. But despite this vast energy resource, harvesting it remains a challenge because of the limited energy conversion efficiency of photovoltaic (PV) panels [1], [2]. Commercially available PV panels have energy conversion efficiencies that range from 14% to 22% [3]. This low efficiency is further aggravated by environmental factors like solar irradiance [3]-[5]. The amount of solar radiation impinging on the PV panel's surface changes with its position. According to [6], solar radiation is at a maximum when the panel is perpendicular to the direct beam of the solar radiation, in effect; PV panels generate the most amount of power [3], [7]-[10]. Deviating from the perpendicular position causes power loss defined by (1) [11]. An increase in the angle of misalignment, θ, decreases the amount of solar radiation received by the panel as shown in Fig. 1.

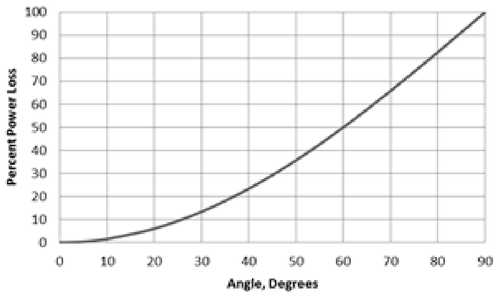

Fig. 1: Direct power loss due to misalignment in angle

$$Power\ Loss = 1 - \cos\theta \quad (1)$$

It is a common sight in the Philippines that PV panels are installed on residential rooftops in a fixed tilted position as a stand-alone system to harvest solar energy. However, a fixed panel setup maximizes direct sun exposure only at particular times of the day. [12] estimated the energy obtained by a fixed system at 8.4KWh/m2, while a PV panel that is always maintained perpendicular to the solar radiation obtained 13.2 KWh/m2. This shows that a fixed system is less efficient at harvesting solar energy during the daytime. To capture the most amount of solar radiation available, solar tracking systems are used. The basic idea is to follow the sun's movement throughout the day and keep the PV panel normal to the direct beam of the solar radiation to maximize power generation. Tracking systems based on their movements are classified into single axis and dual axis trackers [6]. A single axis tracker uses one axis of rotation to orient the panel to an optimal position with the sun. This system utilizes a single motor and significantly improves the reception of available solar radiation as compared with a fixed PV panel [13]. These trackers are beneficial at latitudes close to the equator [11]. In contrast, a dual axis tracker uses two axes of rotation. It can track the sun's azimuth and altitude positions. This system is more accurate but necessitates a more intricate form of control in comparison to a single axis tracker [14].

Tracking systems utilize different control techniques to efficiently track the sun's movement. [15] categorized these techniques into passive and active systems. Passive systems track the sun without electrical devices.

Revised Manuscript Received on 30 July 2019.
* Correspondence Author
Rexel U. Sabran*, Graduate School, Technological Institute of the Philippines-Quezon City, Philippines and Computer Engineering Department, University of San Agustin, Philippines
Arnel C. Fajardo, School of Engineering and Information Technology, Manuel L. Quezon University, Philippines

It operates based on a material's thermal expansion or the difference in pressure of gasses or liquids at opposite points of the tracker.

Passive systems are simple to operate but are less efficient as compared to active systems [12]. On the other hand, active systems continuously track the sun movement using sensors and motors. This technique is fairly accurate in tracking but has difficulties in locating the sun's apparent position during cloudy conditions [6]. Studies conducted by [16]-[18] introduced active tracking systems that use artificial intelligence to drive the solar tracker. Artificial intelligence techniques like neural networks, fuzzy logic, and a combination of both were used to control the tracking system. AI controlled trackers were able to provide efficient and accurate tracking but require data sets and are relatively complex [15].

Solar tracking systems employ different tracking strategies. Solar trackers typically use sun pointing sensors to locate the sun's position with a high degree of accuracy. This form of approach is referred to as the microprocessor and sensor-based tracking strategy [6], [19]. However, this tracking strategy is unreliable [12]. This is mainly due to the weakness innate in sun pointing sensors which are ineffective without the sun and in the strong occurrence of reflected light [20]; and are vulnerable to tracking errors caused by improper installation and effects of varying weather conditions [21]. This, in turn, results in poor tracking performance [22] that undesirably affects the power generation of PV panels.

A sunflower-inspired solar tracking strategy [23] was proposed to address the mentioned weakness. The strategy mimics the solar tracking behavior of a common sunflower that is influenced by the light stimulus and a circadian clock [24]. It uses the light-generated current from the PV panel that works in conjunction with the real time clock module to track the sun's apparent position. The approach provided a good tracking performance with an average tracking error of 0.727° under different weather conditions. The result of the experiment conducted also shows that the strategy maximizes the reception of the available solar radiation by an estimated 99.7%. However, there are instances where the scheme incurred high tracking errors by as much as 1.99° due to false detection brought about by the abrupt changes in the amount of solar radiation. In addition, the proposed strategy also maintains high stepper motor current consumption due to the utilization of a fixed stepping resolution during reorientation.

The goal of this study is to improve the tracking performance of the previous approach under clear, partly cloudy, and cloudy conditions. The key to improving the performance is to direct the search for the sun's position to a range of calculated altitude angles where a fine-tuning process is performed using current measurements. This ensures that the tracker is searching for the sun's position in the correct location. The reduction of the tracking error translates to an improved reception of the available solar radiation, in effect; the PV panel generates more power. The study also seeks to improve the stepper motor current consumption by adopting a variable stepping resolution during tracking. The basic idea of this approach is to minimize the number of steps made by the stepper motor during the realignment process to reduce current consumption. Specifically, the study aims to measure and evaluate:

- the tracking performance of the proposed improvement in terms of tracking error as compared with a reference altitude angle obtained from the National Oceanic and Atmospheric Administration (NOAA) solar calculator and power gained over a fixed tilted panel and;
- the performance of the proposed power saving mechanism in reducing the current consumption of the stepper motor as compared to a fixed stepping resolution approach.

II. METHODOLOGY

A. Tracking Routine

In the previous study, the tracking routine was separated into normal mode and automatic mode. Under the normal mode, a unique way of detecting the sun's position using the current generated by the PV panel was used. It operates based on the fact that maximum solar radiation occurs when the sun's direct beam is perpendicular with the panel. Since the current produced by the PV panel is directly influenced by the solar radiation [25], finding the position that generates the greater current is a good indicator of the perpendicularity of the panel with the sun.

During the process of locating the sun's apparent location, a current reading was taken before realignment. This was compared to succeeding measurements taken after the panel was moved at a fixed step angle of 0.45°. An increase in the current generated by the PV panel halts the realignment process. This indicates that the panel is in the optimal position to harvest solar energy. A problem arises when a sudden increase in the amount of solar radiation occurred during reorientation to a position where the panel is supposedly in parallel with the sun's direct beam. This caused the tracker to falsely detect the perpendicular position of the panel with the sun; as a result, large tracking errors were observed. On the other hand, automatic mode estimates the sun's altitude position using astronomical equations. This tracking mode was intended to operate under cloudy conditions where the current reading is less than or equal to 0.2A, during which, the normal mode fails to detect the sun's location. This approach provided a reliable means of tracking in the absence of the sun [26]. To address the issue of false detection, the tracking routine was modified to include the proposed solution mentioned earlier as shown in Fig. 2. The formula used to calculate the solar angles in this study was derived from the work of [27]. It was specifically chosen because of the simplicity of the required parameters to calculate the solar angles. The routine starts by reading the current time which is necessary for the calculation of the altitude angle. The altitude angle, *Alt_Ang*, is computed using (2). Where δ, φ, and ω are the declination angle, latitude, and hour angle respectively.

$$Alt\_Ang = \sin^{-1}(\sin\delta \ \sin\varphi + \cos\delta \ \sin\varphi \ \cos\omega) \quad (2)$$

To obtain the declination and hour angles, (3)-(7) are used. First, the fractional year, γ, in radians, which defines a position in the earth's orbit around the sun, is computed. The *day_of_year* is the number of the day in a year where January 1 is day 1 and *hour* is the hour of the day in a 24-hour clock.

$$\gamma = (2\pi / 365)[day\_of\_year - 1 + (hour - 12) / 24] \quad (3)$$

Then, the equation of time, *EoT*, given in minutes can be estimated. It is used as a correction factor that accounts the non-uniformity of the earth's speed of motion around the sun.

$$EoT = 229.18\,(0.000075 + 0.001868\cos\gamma - 0.032077\sin\gamma - 0.01461\cos2\gamma - 0.040849\sin2\gamma) \quad (4)$$

From γ, the declination angle, δ, in radians is derived. It is the angle made by the equator and the line that connects the midpoints of the sun and the earth.

$$\delta = 0.006918 - 0.399912\cos\gamma + 0.070257\sin\gamma - 0.006758\cos2\gamma + 0.000907\sin2\gamma - 0.00269\cos3\gamma + 0.00148\sin3\gamma \quad (5)$$

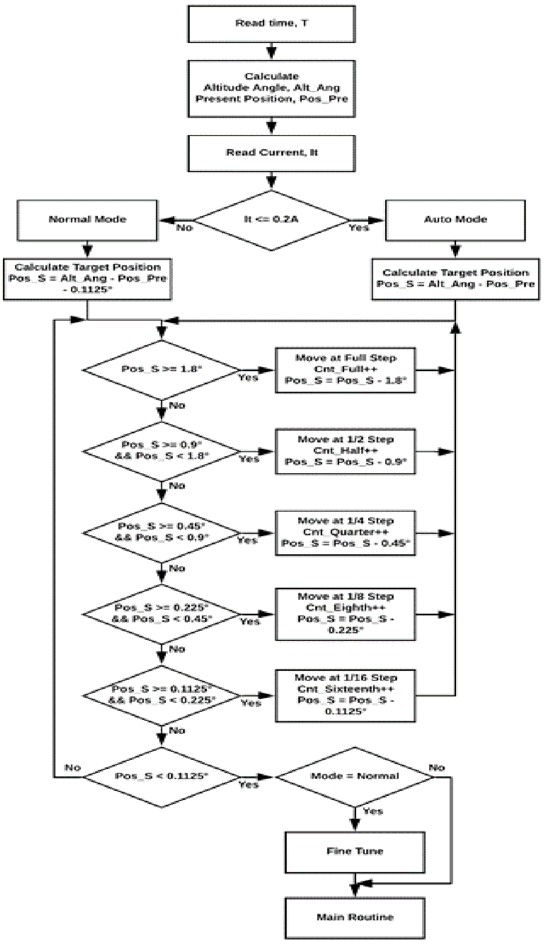

Fig. 2: Modified tracking routine

The true solar time, *tst,* in minutes which is used in forecasting the direction of the sun's rays with respect to a location on earth is then calculated. The *longitude* and *time_zone* refer to the longitude and time zone of the site.

$$tst = [60\,(hour) + minutes + (seconds / 60)] + [EoT + 4\,(longitude) - 60\,(time\_zone)] \quad (6)$$

Next, the hour angle, ω, expressed in degrees is obtained. It denotes the instantaneous position of the sun in the sky.

$$\omega = (tst/4) - 180 \quad (7)$$

The routine then estimates the current position of the PV panel, *Pos_Pre*, using (8). Where, 14.25° is the default inclination of the PV panel with respect to the vertical axis, *Cnt_Full*, *Cnt_Half*, *Cnt_Quarter*, *Cnt_Eighth*, and *Cnt_Sixteenth* are the number of steps made using different stepping resolutions. These counters are initialized to zero at the start of the program.

$$Pos\_Pre = 14.25° + 1.8°\,(Cnt\_Full) + 0.9°\,(Cnt\_Half) + 0.45°\,(Cnt\_Quarter) + 0.225°\,(Cnt\_Eigth) + 0.1125°\,(Cnt\_Sixteenth) \quad (8)$$

Current measurement is then taken to determine which tracking mode will be used. If the current is less than or equal to 0.2A, this indicates a cloudy condition and selects the auto mode. Under this mode, the sun's position is estimated using (9) without the aid of the fine-tuning process. This calculated position represents the midpoint of the fine-tuning scope. On the other hand, a current reading greater than 0.2A will select the normal mode. During which, the starting position where the fine-tuning process will take place is calculated using (10). The 0.1125° in (10) represents the average differences between the calculated solar altitude angles and the reference altitude angles obtained from the NOAA solar calculator. In either case, the modified routine then moves the panel to the starting position with the least number of steps by selecting the appropriate step resolution. Selection of the step resolution is done by providing the mode pins of the DRV8825 stepper motor driver with the proper bit combination. This is a unique power saving mechanism that aims to lower the current consumption of the stepper motor during tracking.

$$Pos\_S = Alt\_Ang - Pos\_Pre \quad (9)$$

$$Pos\_S = Alt\_Ang - Pos\_Pre - 0.1125° \quad (10)$$

The fine-tuning process, as shown in Fig. 3, commences at the calculated starting position. The search for the sun's position begins by comparing the current readings taken from the position before reorientation and the current position. In the event that the present current reading is higher than the previous, the fine-tuning process is exited, otherwise, the panel is moved to the next position. This process is repeated until it has found the position that generates the higher current or has reached the stop position defined by *Alt_Ang – Pos_Pre + 0.1125°* which is equal to two one sixteenth steps from the starting position.

After the tracking routine has realigned the panel to an optimal position to harvest solar energy, program execution is returned back to the main routine as seen in Fig. 4. The tracking routine is executed at intervals of 30 minutes and is halted at sunset.
The panels are then reverted back to its easterly position by reversing the stepper motor rotation in anticipation of the next sunrise.

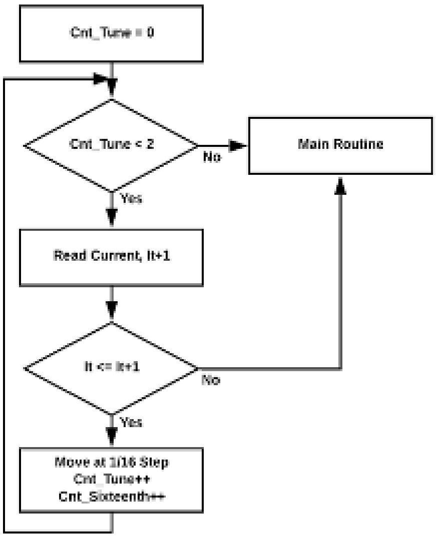

Fig. 3: Fine-tuning routine

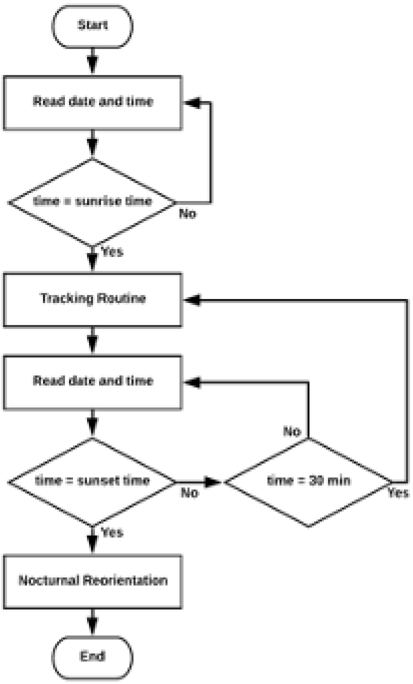

Fig. 4: Main routine

B. Prototype

The hardware components that constitute the single axis solar tracker prototype draws power from a 500W ATX power supply unit. The heart of the system is an Arduino Mega 2560 microcontroller. Signals provided by the microcontroller controls the direction of rotation, stepping resolution, and stepping of a bipolar stepper motor via the DRV8825 driver. Appropriate control signals are generated base on the inputs supplied by the DS3231 real time clock module and the ACS712 current sensor. A program that supervised the tracking operation was developed using the Arduino IDE 1.6.11, keeping the 10W Titan-SI-010 PV panel normal to the solar radiation to maximize power generation.

C. Experimental Setup

The experiments were performed in Iloilo City with a latitude of 10.7202° and longitude of 122.5621°. The site's coordinates and the day of the year were pre-programmed into the microcontroller. Due to the site's geographical makeup that limits the sun's visibility in the early morning and late afternoon, sunrise and sunset times were adjusted to 8:00 am and 4:10 pm respectively. Two identical PV panels were used, one for the fixed tilted setup and another for the tracker. The panel on the tracker was initially directed to face east, rotating along the north-south axes. While the fixed tilted panel was inclined by 8.7° with the horizontal facing south. The panels' orientation is shown in Fig. 5.

Fig. 5: PV panel orientation

The voltage, current, and angle of inclination measurements were taken at 30-minute intervals after panel realignment starting from 8:00 am to 4:00 pm. The voltage and current generated by the PV panels were measured using a digital multimeter and were used to calculate for the power. The angle of inclination made by the tracker was measured using a digital inclinometer with an angle resolution of 0.05°. These angle measurements were compared to a reference altitude angle from the NOAA sun calculator to obtain the tracking error. The average current draw by the stepper motor under different stepping resolution was estimated using the information retrieved from Texas Instruments' DRV8825 datasheet. A table reflecting the relative current ratio supplied to the windings of the motor to achieve different step resolution was used as a basis for the estimation. These estimates were used to project the current consumption of the motor during the tracking operation. To determine the number of steps made using a specific step resolution, a simulation of the tracking routine was developed using MS Excel for the first day of experimentation.

III. RESULTS AND DISCUSSION

The 4-day experiment was conducted last March 23, 24, 27, and 28, 2019. The weather conditions on these dates were mostly clear with occasional partly cloudy to cloudy occurrences. Results of the experiments are categorized into the following:

A. Tracking Error

The tracking errors incurred during the operation are shown in Fig. 6. The highest errors recorded during clear, partly cloudy and cloudy conditions were 0.20°, 0.20°, and 0.24° respectively. The result suggested that the normal mode operating during clear and partly cloudy conditions delivered better accuracy than the auto mode.

This was due to the current measurements providing a direct means of detecting the sun's position, unlike the use of astronomical equations which estimates the position of the sun without any feedback from the environment. In the previous approach, the highest errors were 1.04° for clear, 1.13° for partly cloudy, and 1.99° for the cloudy condition. Differentiating both schemes reveals that the modification in the tracking routine was able to minimize the negative effect of false detection that resulted in lower tracking errors. A comparison between the tracking performance of both the previous and the modified approaches in terms of tracking error, as shown in Table I, reveals that the proposed improvement significantly reduced the overall average tracking error by as much as 84%.

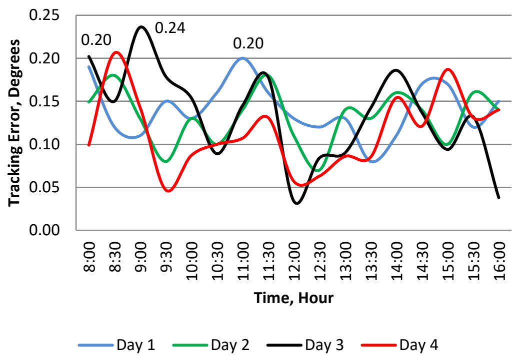

Fig. 6: Measured tracking errors during the 4-day experiment

Table I: Average Tracking Errors Under Different Weather Conditions

Weather Condition	Clear	Partly Cloudy	Cloudy	Overall Average Tracking Error
Previous	0.503°	0.687°	0.956°	0.727°
Modified	0.124°	0.143°	0.191°	0.114°

B. Power Generation

The powers generated by the PV panels are shown in Fig. 7 to Fig. 10. It clearly showed the distinct advantage of solar tracking systems in maximizing the harvesting of solar energy as compared to a fixed tilted system. This was observed during the early morning and afternoon where the tracker orients the panel to an optimal position to generate electricity. However, in a cloudy condition, both panels were severely affected by the momentary absence of the sun where the power generated by the panels drastically drops to as low as 0.82W. At noon, when the sun is more or less directly overhead, a slight difference in power generated between the panels was observed. This is due to that the fixed tilted panel is also in the optimal position to maximize power generation. Overall, the tracking system was able to produce an average of 23.58% more power as compared to a fixed tilted system. In contrast, the previous approach achieved an average of 20.5% power gain over a fixed system. Comparing both, the modified scheme produced 3.08% more power. As a result of reducing the tracking error, an improvement in the power gain of 15% was achieved.

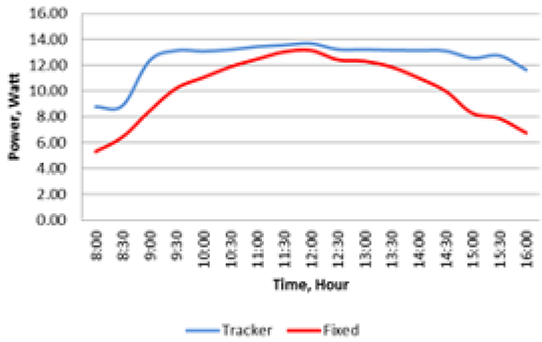

Fig. 7: The power generated by the tracker and fixed panel on Day 1

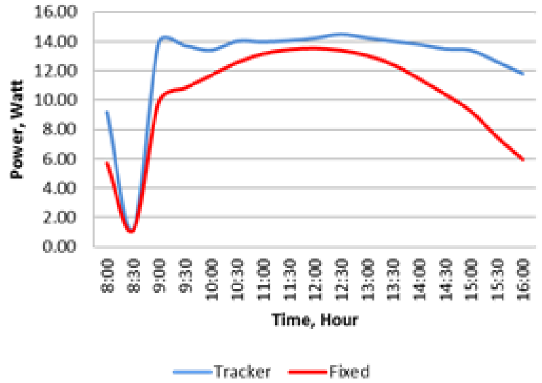

Fig. 8: The power generated by the tracker and fixed panel on Day 2

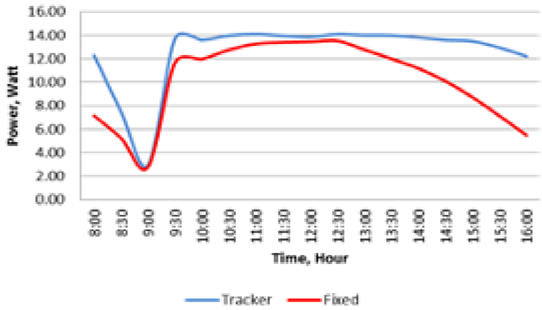

Fig. 9: The power generated by the tracker and fixed panel on Day 3

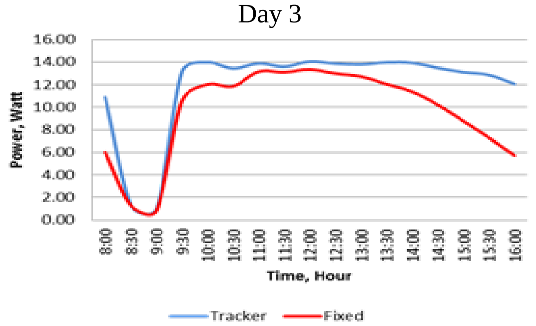

Fig. 10: The power generated by the tracker and fixed panel on Day 4

C. Stepper Motor Current Consumption

Table II shows the estimated average current consumed by the stepper motor at different stepping resolutions base on a 1.0A per winding reference. From these estimates, a projection of the total current consumption of the stepper motor during tracking was obtained for the fixed stepping angle approach and the proposed variable stepping angle as seen in Table III.

In the previous study, the panel was moved at a constant stepping resolution of 0.45°. Reorienting the panel in this way requires a considerable number of steps to reach a targeted position, consequently, consuming more current. Varying the stepping resolution during the realignment process resulted in a lesser number of steps, in effect, reducing the current consumption of the motor. A comparison of the projected average current draw of the stepper motor during tracking between the previous and the modified schemes showed that the proposed modification reduces the current consumption by an estimated 53%.

Table II: Average Current Consumption at Different Step Resolutions

Step Resolution	Average Current Draw per Step
Full	1.42A
Half	1.14A
Quarter	1.20A
One Eigth	1.22A
One Sixteenth	1.24A

The performance of the previous and modified approaches is summarized in Table IV. This shows that modifications introduced in the tracking routine demonstrated a significant improvement in the average tracking error under clear, partly cloudy, and cloudy weather conditions. Improvement in the overall average tracking error resulted in an increase in power generated. Moreover, the adoption of a variable stepping resolution during the realignment process was projected to improve the current consumption of the stepper motor in comparison to a fixed stepping angle approach used in the previous study.

Table III: Projected Current Consumption for Day 1

Calculated Target Position, Degrees	Number of Steps						Current Consumption During Reorientation, Ampere	
	Modified					Previous		
	1.8°	0.9°	0.45°	0.225°	0.1125°	0.45°	Modified	Previous
16.03	8	1	1		2	35	16.18	42.00
7.61	4				2	16	8.16	19.20
7.70	3	1	1	1	3	17	11.54	20.40
7.28	3	1	1	1	2	16	10.30	19.20
7.20	3	1	1		3	15	10.32	18.00
7.37	3	1	1		2	16	9.08	19.20
6.66	3	1			2	14	7.88	16.80
5.65	2	1	1		3	12	8.90	14.40
22.32	12			1	1	49	19.50	58.80
3.17	1	1			3	7	6.28	8.40
5.67	3					12	4.26	14.40
6.87	3	1		1	2	15	10.34	18.00
7.09	3	1	1			15	6.60	18.00
7.49	3	1	1	1	2	16	10.30	19.20
7.53	3	1	1	1	2	16	10.30	19.20
7.63	4				2	16	8.16	19.20
7.76	3	1	1	1	2	17	10.30	20.40
Projected average current consumption during tracking							9.91	21.46

Table IV: Summary of Performance

Schemes	Average Tracking Error, Degrees				Percent Power Gain over a Fixed Tilted Panel	Projected Current Consumption During Tracking, Ampere
	Clear	Partly Cloudy	Cloudy	Overall		
Previous	0.503	0.687	0.956	0.727	20.50%	21.46
Modified	0.124	0.143	0.191	0.114	23.58%	9.91
Improvement over Previous Study	75.35%	79.18%	80.02%	84.32%	15.02%	53.82%

IV. CONCLUSION AND FUTURE WORK

Modifications introduced to the tracking routine of the sunflower-inspired solar tracking strategy were intended to improve the tracking error and stepper motor current consumption. A series of experiments were conducted to measure the performance of the modifications in terms of tracking error, power generation, and stepper motor current consumption. The results showed that by directing the fine-tuning process to a range of altitude angles where the sun is perceived to be, reduced the average tracking error by as much as 84%. In effect, increasing the power generated by 15% as compared with the previous scheme. The result of the simulation also showed that the use of a variable stepping resolution during reorientation projected a reduction in the total average motor current consumption by an estimated 53% in contrast to a fixed stepping resolution approach. Thus, the proposed modifications significantly improved the overall tracking performance of the strategy. The otential of the proposed power saving mechanism is promising. This warrants further investigation that will consider the actual current draw of the stepper motor during tracking in order to obtain the concrete savings in current consumption. The proposed tracking strategy is currently applied to drive a single panel of a stand-alone PV system in a residential setting. Future work will investigate the use of this approach to efficiently and accurately drive an array of panels for residential PV applications.

ACKNOWLEDGMENT

R. Sabran would like to thank the University of San Agustin and the Commission on Higher Education of the Philippines for their support.

REFERENCES

1. K.Y. Lee, C.Y. Chung, B.J. Huang, T.J. Kuo, H.W. Yang, H.Y. Cheng, P.C. Hsu, and K. Li, "A novel algorithm for single-axis maximum power generation sun trackers," Energy Conversion and Management, Vol. 149, 2017, pp. 543-552.
2. T. Kaur, S. Mahajan, S. Verma, Priyanka, and J. Gambhir, "Arduino based low cost active dual axis solar tracker," 2016 IEEE 1st International Conference on Power Electronics, Intelligent Control and Energy Systems (ICPEICES), Delhi, 2016, pp. 1-5.
3. M. Fouad, L. Shihata, and E. Morgan, "An integrated review of factors influencing the performance of photovoltaic panels," Renewable and Sustainable Energy Reviews, Vol. 80, 2017, pp. 1499-1511.
4. A. Syafiq, A. Pandey, N. Adzman, and N. Rahim, "Advances in approaches and methods for self-cleaning of solar photovoltaic panels," Solar Energy, Vol. 162, 2018, pp. 597-619.
5. Shefali, H. Singh, S. Kumar, and I. Kaur, "Designing and simulation of solar module in the islanded network of solar PV microgrid," International Journal of Recent Technology and Engineering (IJRTE), Vol. 7, Issue 6S4, 2019, pp. 254-258.
6. W. Nsengiyumva, S. Chen, L. Hu, and X. Chen, "Recent advancements and challenges in Solar Tracking Systems (STS): A review," Renewable and Sustainable Energy Reviews, Vol. 81, Part 1, 2018, pp. 250-279.
7. P. Junaidh, A. Vijay and M. Mathew, "Power enhancement of solar photovoltaic module using micro-climatic strategies in warm-humid tropical climate," 2017 Innovations in Power and Advanced Computing Technologies (i-PACT), Vellore, 2017, pp. 1-6.
8. S. Aziz and S. Hassan, "On Improving the Efficiency of a Solar Panel Tracking System," Procedia Manufacturing, Vol. 7, 2017, pp. 218-224.
9. W. Batayneh, A. Owais, and M. Nairoukh, "An intelligent fuzzy

based tracking controller for a dual-axis solar PV system," Automation in Construction, Vol. 29, 2013, pp. 100-106.
10. S. M. Jalil et al., "Solar cell position control building design using microcontroller for optimizing power sunway in the coffee drying application," International Journal of Recent Technology and Engineering (IJRTE), Vol. 7, Issue 6S5, 2019, pp. 1490-1496.
11. M. Tania and M. Alam, "Sun tracking schemes for photovoltaic panels," 2014 3rd International Conference on the Developments in Renewable Energy Technology (ICDRET), Dhaka, 2014, pp. 1-5.
12. H. Mousazadeh et al., "A review of principle and sun-tracking methods for maximizing solar systems output," Renewable and Sustainable Energy Reviews, Vol. 13, Issue 8, 2009, pp. 1800-1818.
13. M. Rahul, P. Baredar, and B. Gupta. "Analysis of Tracking Mechanism for PV System," International Journal of Advanced Research in Computer Science and Electronics Engineering (IJARCSEE), 2014, pp. 253-257.
14. V. Sumathi, R. Jayapragash, A. Bakshi, and P. Akella, "Solar tracking methods to maximize PV system output – A review of the methods adopted in recent decade," Renewable and Sustainable Energy Reviews, Vol. 74, 2017, pp. 130-138.
15. N. AL-Rousan, N. Isa, and M. Desa, "Advances in solar photovoltaic tracking systems: A review," Renewable and Sustainable Energy Reviews, Vol. 82, Part 3, 2018, pp. 2548-2569.
16. A. Zaher, N'G. Yao, and A. Traore, "Fuzzy rule-based model for optimum orientation of solar panels using satellite image processing," IOP Conference Series: Journal of Physics, 2017.
17. A. Aldair, A. Obed, and A. Halihal, "Design and implementation of Neuro-Fuzzy controller using FPGA for sun tracking system," Iraqi Journal for Electrical and Electronic Engineering, Vol. 12, Issue 2, 2016, pp. 123-136.
18. M. Panait and T. Tudorache, "A simple neural network solar tracker for optimizing conversion efficiency in off-grid solar generators," In: Proceedings of international conference on renewable energies and power quality, 2008.
19. R. Singh, S. Kumar, A. Gehlot, and R. Pachauri, "An imperative role of sun trackers in photovoltaic technology: A review," Renewable and Sustainable Energy Reviews, Vol. 82, Part 3, 2018, pp. 3263-3278.
20. A. Shintemirov et al., "A sensorless MPPT-based solar tracking control approach for mobile autonomous systems," IECON 2016 - 42nd Annual Conference of the IEEE Industrial Electronics Society, Florence, 2016, pp. 3006-3011.
21. L. Salgado-Conrado, "A review on sun position sensors used in solar applications," Renewable and Sustainable Energy Reviews, Vol. 82, Part 3, 2018, pp. 2128-2146.
22. Y. Yao, Y. Hu, S. Gao, G. Yang, and J. Du, "A multipurpose dual-axis solar tracker with two tracking strategies," Renewable Energy, Vol. 72, 2014, pp. 88-98.
23. R. Sabran and A. Fajardo, "Sunflower Inspired Solar Tracking Strategy: A Sensorless Approach for Maximizing Photovoltaic Panel Energy Generation," 2018 IEEE 10th International Conference on Humanoid, Nanotechnology, Information Technology, Communication and Control, Environment and Management (HNICEM), Baguio City, Philippines, 2018, pp. 1-6.
24. H. Atamian, N. Creux, E. Brown, A.G. Garner, B. Blackman, and S. Harmer, "Circadian regulation of sunflower heliotropism, floral orientation, and pollinator visits," Science 353, 2016, pp. 587-590.
25. M. G. Villalva, J. R. Gazoli and E. R. Filho, "Comprehensive Approach to Modeling and Simulation of Photovoltaic Arrays," in IEEE Transactions on Power Electronics, vol. 24, no. 5, 2009, pp. 1198-1208.
26. H. Fathabadi, "Novel high efficient offline sensorless dual-axis solar tracker for using in photovoltaic systems and solar concentrators," Renewable Energy, Vol. 95, 2016, pp. 485-494.
27. A. Merlaud, M. De Mazière, C. Hermans, and A. Cornet, "Equations for solar tracking," Sensors, Vol. 12, 2012, pp. 4074-4090.

AUTHORS PROFILE

Rexel U. Sabran obtained his Bachelor of Science degree in Computer Engineering from Western Institute of Technology, Philippines in 1999. He finished his Master's degree in Engineering from the same institution in 2004. He is currently taking up Doctor of Engineering with specialization in Computer Engineering from the Technological Institute of the Philippines – Quezon City. His research interests include biomimetics and renewable energy.

Arnel C. Fajardo received his B.S. Electrical Engineering degree in 1991 from the Mapua Institute of Technology in Intramuros, Manila. He obtained his M.S. Computer Science degree in 1999 from De La Salle University Manila. He obtained his Ph.D. in Computer Engineering degree from Hanbat National University, Daejon, South Korea in 2014. He is the Senior Assistant Vice President and Research Director of Manuel L. Quezon University and Professorial lecturer of various universities in the Philippines. He is an author of more than 30 articles in journals and conference proceedings. His research interest includes speech recognition, image processing, artificial intelligence, and engineering education.